Liquid-Crystal-Embedded Aperture-Coupled Microstrip Antenna for 5G Applications

Jaehoon Kim, *Student Member, IEEE*, and Jungsuek Oh, *Senior Member, IEEE*

***Abstract*—This letter presents a novel reconfigurable microstrip antenna with a frequency of 28 GHz and an embedded liquid crystal (LC). First, a novel fabrication process that employs a heat press machine is developed. This allows for the successful creation of thin substrates with thicknesses ranging between 0.13 and 0.25 mm. It is validated that the proposed stacked topology achieves a wide tunable range of resonant frequency. In addition, a simple bias configuration is achieved by connecting the bias position to the middle of the patch, where radio frequency (RF) potential is zero. The proposed antenna adopts a three-layer stacked printed circuit board (PCB) structure to render a cavity in which the LC is injected. The bottom patch of the top substrate is designed to contact the LC, and thus, it simultaneously functions as a dc bias electrode and a radiating element. In addition, unlike conventional stacked patch antennas, the additional patch on the top of the PCB structure is tuned to enhance gain. Compared with the simulated performance of a prior LC-based antenna, the tunable range of the resonant frequency of the proposed antenna is improved by more than three times at a center frequency of 28 GHz and the peak radiation efficiency is improved by up to 17%. Furthermore, the area (252 mm^2) of the proposed LC-based antenna is 40% of the area of the prior LC-based antenna (625 mm^2).**

***Index Terms*—Liquid crystals (LCs), microstrip antennas, millimeter-wave antennas, reconfigurable antennas.**

I. Introduction

In 5G communication era, the implementation of millimeter-wave antennas is challenging in terms of not only structural integration but also inherent performance, such as beam coverage and bandwidth. In particular, the range of the frequency bands being considered for millimeter-wave 5G is increasing continuously. For example, the 28 GHz band employed only approximately 1 GHz five years ago but currently extends up to 3 GHz or more. Furthermore, the design conditions for millimeter-wave 5G antennas are becoming more stringent. A small form factor and a low-profile structure are required to efficiently integrate these antennas with beamforming ICs. In the millimeter-wave band, numerous works have investigated the reconfigurable antenna technology for various types of tunable elements to support wideband performance at a limited physical antenna volume [1]–[3]. Such antenna technologies have typically employed p-i-n diodes, varactors, and liquid crystals (LCs). Among these, LCs provide advantages over other reconfigurable elements at millimeter-wave frequencies. LCs provide low loss at high frequencies. Moreover, they can be inserted inside antennas, while p-i-n diodes and varactors are mounted on the top of antenna planes and lead to a protruded and large-sized outer appearance. Despite these advantages of LCs, most studies on existing LC-based antennas have not reported measurement results [4]–[6]. A few works have reported the tunable range of the dielectric constant of LCs. The loss features of LCs are extremely poor in microwave frequency bands [7], [9]. The aforementioned studies have not discussed the possibility of developing a new process of manufacturing an antenna structure that can be applied to 5G communication [8]–[11].

In this letter, a novel LC-based low-profile stacked PCB antenna with a wide reconfigurable frequency range is proposed. To the best of our knowledge, LC-based planar antennas with thickness similar to that of the proposed low-profile antenna have not yet been fabricated owing to the bending and alignment issues of thinly stacked PCBs. The thin and stable configuration of the proposed antenna is achieved by utilizing a compression manufacturing process, which employs a heat press machine and a water-resistant epoxy to prevent the leakage of the LC. The rest of this letter is organized as follows. Section II presents the novel antenna configuration, which employs a simple biasing scheme, and the thin PCB-based antenna stack up the fabrication process. Section III describes the simulation and measurement results obtained using the fabricated antenna. Finally, Section IV presents the conclusions.

II. Antenna Design and Fabrication

This section describes the antenna configuration, which comprises a simple compact biasing scheme and a fabrication process that uses a heat press machine. The antenna is designed at 28 GHz, and its dimensions are 18 mm (lateral dimension along the y-axis) $\times$ 14 mm (lateral dimension along the x-axis) $\times$ 0.65 mm (total thickness), as shown in Fig. 1. The first layer is a microstrip line, which contains a pad and metallic vias for RF transition from a coaxial connector. The ground metal is etched to render an H-shaped slot for a patch to be excited in the third layer. The second layer consists of a milled dielectric, which renders a cavity in the middle to trap the LC. The height of the dielectric is as low as 0.13 mm considering the moderate range of applied dc voltage based on the fact that the required

Manuscript received July 15, 2020; accepted July 29, 2020. Date of publication August 6, 2020; date of current version November 23, 2020. This work was supported in part by the Research Resettlement Fund for the new faculty of Seoul National University and in part by SAMSUNG Research, Samsung Electronics Co., Ltd. *(Corresponding author: Jungsuek Oh.)*

The authors are with the Institute of New Media and Communications and Department of Electrical and Computer Engineering, Seoul National University, Seoul 08826, South Korea (e-mail: jaehoonkim@snu.ac.kr; jungsuek@snu.ac.kr).

Digital Object Identifier 10.1109/LAWP.2020.3014715

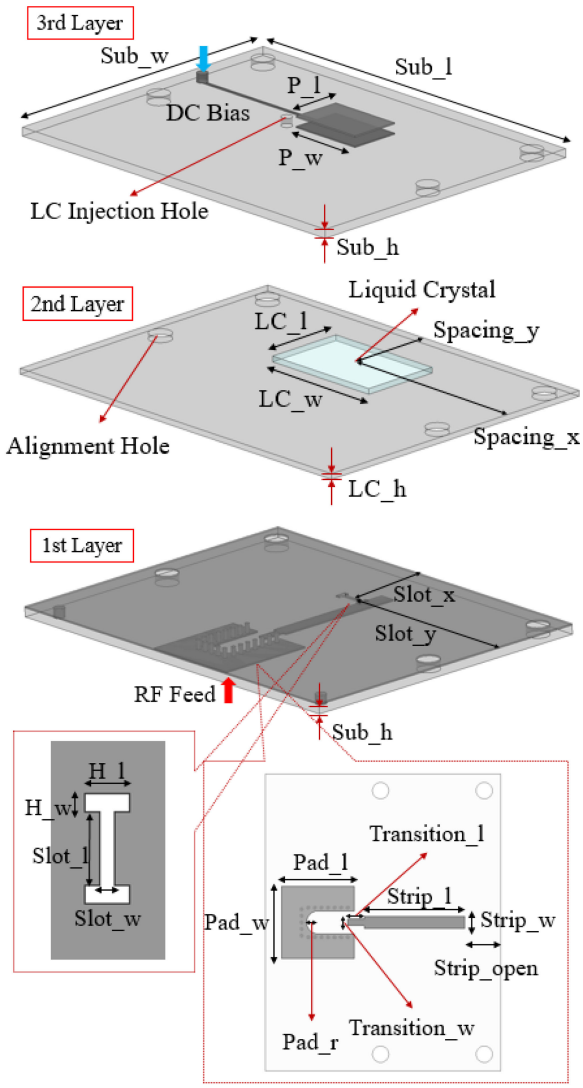

Fig. 1. Exploded view and dimension parameters of the proposed antenna incorporating RF feed and dc bias structure.

maximum dc voltage is proportional to the thickness of the LC layer. According to existing literature [13], [14], a voltage of approximately 20 V is required for the maximum tuning of the LC layer, which has a height of 100 μm. The third layer is a PCB. It consists of stacked patches and functions as a cover for the LC. A fundamental rectangular patch is placed underneath a substrate, and an additional patch for gain enhancement is placed above the substrate. In the middle of the side edge of the bottom patch, a metallic line is connected for dc bias and exposed to the outside for dc excitation. The Taconic TLY dielectric is utilized in all layers, and its dielectric constant and loss tangent are 2.2 and 0.0009, respectively. The LC is injected into the milled cavity in the second layer, and the dielectric constant is tuned based on the applied dc voltage. Based on the datasheet, the tunable range of the dielectric constant is expected to be 2.5–3.5, and the corresponding loss tangent decreased from 0.0116 to 0.0064. There are four via holes for the alignment at the edge of each layer of the antenna, and the diameter of each hole is 1 mm. The diameter of the 19 vias of the RF transition pad is 0.2 mm,

TABLE I
DIMENSION PARAMETERS AND THEIR VALUES FOR THE PROPOSED ANTENNA

3rd Layer					
Sub_l	14.1	Sub_w	18	Sub_h	0.25
P_l	2.32	P_w	3.5		
2nd Layer					
LC_l	3.6	LC_w	5.55	LC_h	0.13
Spacing_x	9	Spacing_y	4		
1st Layer					
Pad_l	4.4	Pad_w	4.4	Pad_r	0.7
Slot_x	9	Slot_y	4	Slot_l	1.05
Slot_w	0.1	Transition_l	1	Transition_w	0.4
H_l	0.5	H_w	0.2	Sub_h	0.25
Strip_l	6	Strip_w	0.73	Strip_open	2.1

(Unit:mm).

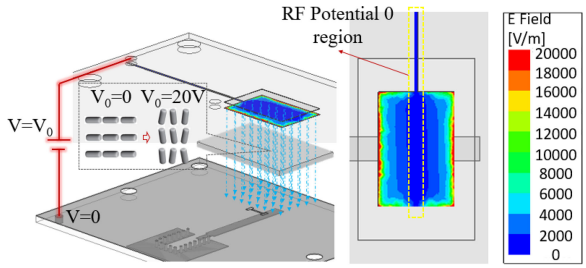

Fig. 2. (a) Conceptual drawings of dc bias configuration and LC molecular state and (b) magnitude of electric field intensity on antenna patch.

and that of the signal and ground vias for applying dc bias is 0.5 mm. The dimension parameters of the proposed antenna are listed in Table I.

A. DC Bias Configuration

To tune the LC in the second layer, LC molecules must be arranged based on potential difference. A simplified antenna topology is achieved by making the ground plane function as the RF and dc ground. The radiation patch underneath the substrate is used to control dc bias, whose potential varies from 0 to 20 V. Fig. 2(a) shows the conceptual drawings of the dc bias configuration and the LC molecular state. As the dc bias circuit should not affect the RF signal, it must not flow into the dc path. There are a few methods for achieving this, such as mounting an inductor chip with a large inductance. However, for creating a simple topology without an additional protruded chip, the dc path is connected to the middle of the patch. Fig. 2(b) depicts the magnitude of the simulated electric field applied to the patch at the operating frequency using the Ansys HFSS full-wave simulator. As the electric potential is zero in the middle part of the resonant patch, connecting a dc bias line to this region does not affect the antenna operation.

B. Fabrication Process and Antenna Sample

Fig. 3 presents a flowchart for the fabrication process of the proposed antenna. In the process, after manufacturing the three-layer PCB, polyimide is coated on the first and third

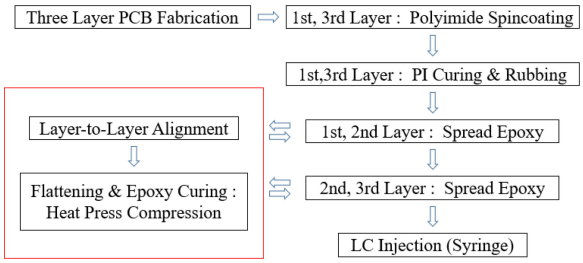

Fig. 3. Flowchart for the fabrication process of the proposed antenna.

(a) (b)

Fig. 4. (a) Spread of polyimide layer through spin coating and (b) rubbing for stable arrangement of LC molecules.

layers for the rubbing process. It should be noted that carving rubbing grains can change the arrangement of LC molecules in a stable manner. In this sense, the value of the dielectric constant can return to the initial condition when applied dc voltage becomes zero. Polyimide is cured under the required temperature condition after it is spread thinly. The alignment process must be performed on the top and bottom substrates that contact the LC to obtain an initial arrangement of irregular LC molecules.

Fig. 4(a) illustrates the spreading of the thin polyimide layer through the spin coating process. A chuck is rotated after placing the polyimide liquid on the antenna. Then, the polyimide liquid spreads thinly. The polyimide layer is cured at a specific temperature condition, and then, rubbing grains are created using a velvet cloth, as shown in Fig. 4(b). The heat press machine allows for the stable fabrication of thin and flat LC-embedded stacked PCB patch antennas under the optimized conditions of adhesion pressure and curing temperature depending on the epoxy type and the degree of thickness. A liquid thermosetting epoxy, which is spread thinly, is used to combine the three substrates. A water-resistant epoxy is used to prevent the leakage of the LC. Fig. 5(a) shows the fabrication process using the heat press machine, and Fig. 5(b) shows the top and bottom views of the fabricated antenna sample. Once the fabrication of the stacked PCB is completed, the LC is injected into the cavity through the LC injection hole drilled in the third layer. The GT7 LC (Merck KGaA) is used in this letter. The LC is injected into the second layer using a syringe [12].

III. Simulation and Measurement Results

Fig. 6 shows the measured dielectric constant of the LC as a function of dc bias voltage. The dielectric constant is calculated

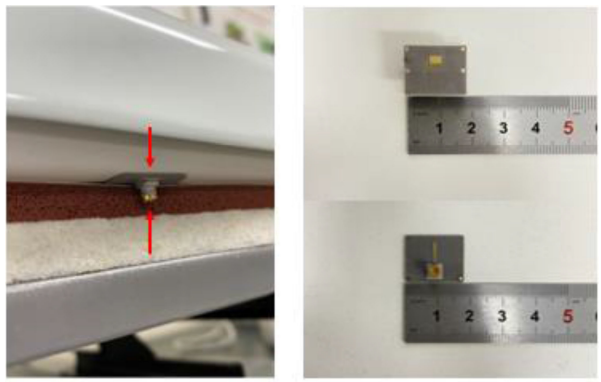

(a) (b)

Fig. 5. (a) Substrate-to-substrate adhesion process using a heat press machine and (b) top and bottom views of the fabricated antenna sample.

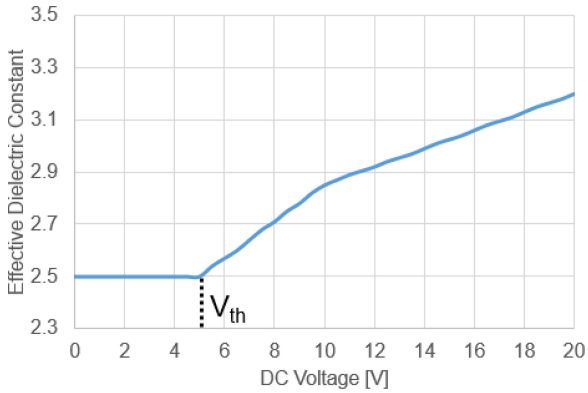

Fig. 6. Effective dielectric constant of LC as a function of dc bias voltage.

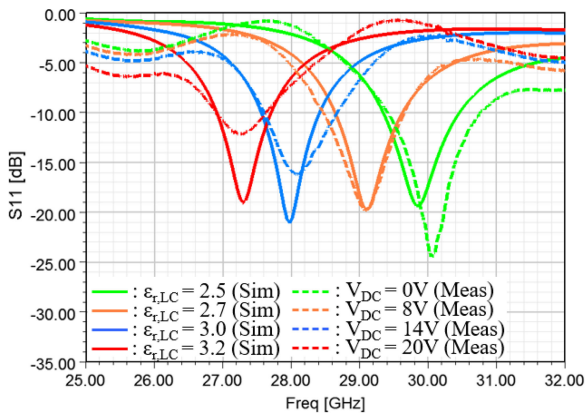

Fig. 7. Comparison between measured S_{11} as a function of dc bias voltage and simulated S_{11} as a function of dielectric constant of LC.

by comparing the simulated S_{11} as a function of the dielectric constant of the LC and the measured S_{11} as a function of dc bias voltage; the comparison is shown in Fig. 7. A dielectric constant over 3.2 is not obtained because of several fabrication issues, such as irregular hands on the rubbing process or damage to the rubbing plain caused by the high temperature of the heat press machine. As dc bias voltage increases, the LC molecules are arranged vertically, leading to an increase in the dielectric

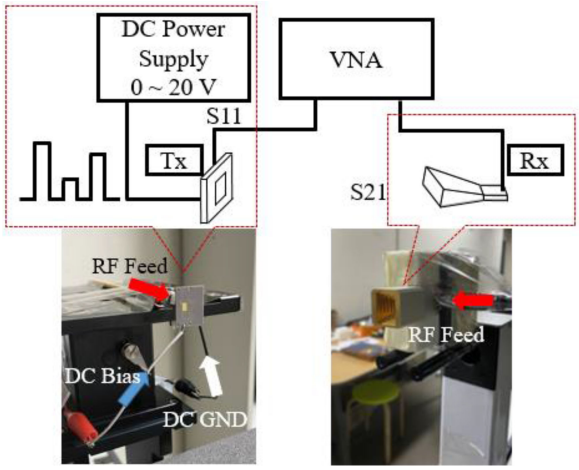

Fig. 8. Conceptual diagram and photographs of the antenna measurement setup.

TABLE II
COMPARISON BETWEEN THE PROPOSED AND PRIOR ANTENNAS

	Tunable range of resonant frequency at 28 GHz	Range of radiation efficiency	Simulated gain (dBi)	Measured gain (dBi)
Prior antenna in [1]	3.1%	3 - 70 %	6.5	Not fabricated
Proposed antenna	10%	78 - 83%	6.5	3.9

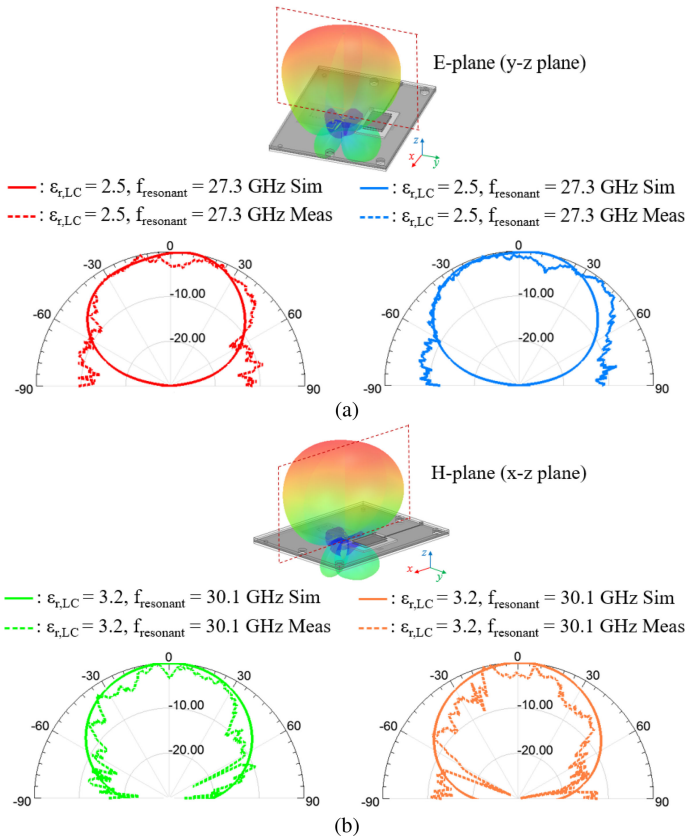

Fig. 9. Comparison between (a) simulation and (b) measurement results of the normalized radiation pattern in the *E*-plane when the resonant frequency of the proposed antenna is tuned to two values.

constant of the LC. Accordingly, the effective wavelength decreases and the antenna becomes relatively large. This reduces the resonant frequency of the antenna. A prior work [1] used the K15 LC (Merck). The properties of this LC are as follows: $\varepsilon_{r,\parallel} = 3.1$, $\varepsilon_{r,\perp} = 2.7$, and loss tangents of $\tan\delta_{\parallel} = 0.0132$ and $\tan\delta_{\perp} = 0.0273$. The range of the dielectric constant utilized in this letter is only 2.72–2.9. As there is no existing literature that presents the measurement results of the reconfigurable bandwidth and tunable range of LC-based microstrip antennas, the measurement results obtained using the proposed antenna are compared with simulated results of the prior work [1].

Fig. 8 shows the system configuration for performing measurements using the proposed antenna. In the measurement setup, a standard horn antenna is used as a receiver antenna. It is connected to one port of a vector network analyzer, and the other port is connected to the LC antenna. Measurements are performed by applying dc voltage to the LC antenna using a dc power supply. The range of applied voltage is 0–20 V, and the threshold voltage is 5 V. Fig. 9 shows the normalized simulated and measured radiation patterns of the proposed antenna in the *E*-plane and *H*-plane. The radiation patterns are measured at two resonant frequencies realized by applying different dc bias voltages. The performance features of the proposed and prior [1] antennas are listed in Table II. The tunable range of the resonant frequency of the proposed antenna is improved by more than three times at a center frequency of 28 GHz. Additionally, the peak radiation efficiency of the proposed antenna is improved by up to 13%. The area (252 mm^2) of the proposed LC-based antenna is only 40% of the area of the prior antenna (625 mm^2). The peak measurement gain is 3.9 dBi, which is lower than the simulated gain of 6.5 dBi. This is because of the connector and feed losses of 1–2 dB at 28 GHz and fabrication errors in the overall thickness and flatness.

IV. CONCLUSION

This letter presents a low-profile 28 GHz aperture-coupled microstrip patch antenna that employs an LC for a wide reconfigurable frequency range. It should be noted that the stacked PCB-based LC antenna proposed in previous work [1] could not be fabricated. A simple antenna topology and a novel fabrication method are presented to overcome the critical challenges in the fabrication of the low-profile LC-embedded antenna. The proposed antenna is compared with the previously developed antenna. The tunable range of the dielectric constant of the LC used in this study is wider, and its loss tangent is lower. This suggests that in the future, the continuous improvement of the RF performance of the LC will allow for the utilization of reconfigurable materials for cutting-edge antenna applications, such as 5G communication. This letter demonstrates that a more sophisticated antenna topology and fabrication method can overcome structural and performance limits in millimeter-wave 5G stacked PCB antennas that use new reconfigurable materials.

REFERENCES

[1] J.-W. Dai, H.-L. Peng, Y.-P. Zhang, and J.-F. Mao, "A novel tunable microstrip patch antenna using liquid crystal," *Prog. Electromagn. Res. C*, vol. 71, pp. 101–109, Jan. 2017, doi: 10.2528/PIERC16120501.

[2] A. E. Hajj Hassan, N. Fadlallah, G. El Nashef, M. Rammal, and E. Rachid, "Compact reconfigurable stacked patch antenna using liquid crystal for 5G networks," in *Proc. 2nd IEEE Middle East North Commun. Conf.*, Manama, Bahrain, 2019, pp. 1–4.

[3] M. Nestoros, N. C. Papanicolaou, and A. C. Polycarpou, "Design of beam-steerable array for 5G applications using tunable liquid-crystal phase shifters," in *Proc. 13th Eur. Conf. Antennas Propag.*, Krakow, Poland, 2019, pp. 1–4.

[4] M. A. Christou, N. C. Papanicolaou, and A. C. Polycarpou, "A nematic liquid crystal tunable patch antenna," in *Proc. 8th Eur. Conf. Antennas Propag.*, Hague, The Netherlands, 2014, pp. 1875–1878.

[5] Y. Zhao, C. Huang, A. Qing, and X. Luo, "A frequency and pattern reconfigurable antenna array Based on liquid crystal technology," *IEEE Photon. J.*, vol. 9, no. 3, Jun. 2017, Art. no. 4600307.

[6] A. C. Polycarpou, M. A. Christou, and N. C. Papanicolaou, "Tunable patch antenna printed on a biased nematic liquid crystal cell," *IEEE Trans. Antennas Propag.*, vol. 62, no. 10, pp. 4980–4987, Oct. 2014.

[7] C. D. Woehrle, D. T. Doyle, S. A. Lane, and C. G. Christodoulou, "Space radiation environment testing of liquid crystal phase shifter devices," *IEEE Antennas Wireless Propag. Lett.*, vol. 15, pp. 1923–1926, 2016.

[8] T.-W. Kim, J.-S. Park, and S.-O. Park, "A theoretical model for resonant frequency and radiation pattern on rectangular microstrip patch antenna on liquid crystal substrate," *IEEE Trans. Antennas Propag.*, vol. 66, no. 9, pp. 4533–4540, Sep. 2018.

[9] O. H. Karabey, A. Mehmood, M. Ayluctarhan, H. Braun, M. Letz, and R. Jakoby, "Liquid crystal based phased array antenna with improved beam scanning capability," *Electron. Lett.*, vol. 50, no. 6, pp. 426–428, Mar. 2014, doi: 10.1049/el.2014.0269.

[10] N. C. Papanicolaou, M. A. Christou, and A. C. Polycarpou, "Frequency-agile microstrip patch antenna on a biased liquid crystal substrate," *Electron. Lett.*, vol. 51, no. 3, pp. 202–204, Feb. 2015, doi: 10.1049/el.2014.3856.

[11] L. Liu and R. J. Langley, "Liquid crystal tunable microstrip patch antenna," *Electron. Lett.*, vol. 44, no. 20, pp. 1179–1180, Sep. 2008, doi: 10.1049/el:20081995.

[12] A. Manabe, "Liquid crystals for microwave applications," in *Proc. 7th Eur. Conf. Antennas Propag.*, Gothenburg, Sweden, 2013, pp. 1793–1794.

[13] S. Bildik *et al.*, "Recent advances on liquid crystal based reconfigurable antenna arrays," presented at the *ESA Workshop on Large Deployable Antennas*, Noordwijk, The Netherlands, Oct. 2–3, 2012.

[14] A. Gaebler *et al.*, "Liquid crystal-reconfigurable antenna concepts for space applications at microwave and millimeter waves," *Int. J. Antennas Propag.*, vol. 2009, Feb. 2009, Art. no. 876989, doi: 10.1155/2009/876989.